# Supporting Information

# Bilayer Molecular Electronics: All-carbon electronic junctions containing molecular bilayers made with "click" chemistry

Sayed Youssef Sayed[1,2,§], Akhtar Bayat[1,2,§], Mykola Kondratenko[1,2], Yann Leroux[3], Philippe Hapiot[3], Richard L. McCreery[1,2*]

1. Department of Chemistry, University of Alberta, Edmonton, Alberta, Canada

2. National Institute for Nanotechnology, National Research Council Canada, Edmonton, Alberta, Canada

3. Sciences Chimiques de Rennes (Equipe MaCSE), CNRS, UMR 6226, Université de Rennes, France

[§]These authors contributed equally to this work.

*corresponding author: richard.McCreery@ualberta.ca

# Experimental:

## Reagents and chemicals

Acetonitrile (ACN), acetone, isopropanol (IPA), triethylamine (TEA) and $CuSO_4$ x $5H_2O$ were used as received from Fischer Scientific. Tetrahydrofuran (THF) was acquired from Caledon. Ascorbic acid, benzene, and ammonium hydroxide were received from EMD. Anhydrous ethanol was purchased from Green Field Ethanol Inc. All other chemicals were purchased from Sigma-Aldrich and used without further purification.

Azidomethylferrocene (MeFc),[1] azidohexylferrocene (HxFc),[2] 1-azidooctane ($C_8$ azide),[3] 1-azidododecane (C12 azide)[3], 1-azidohexadecane ($C_{16}$ azide)[4], 4-Ethynylbenzene (EB) diazonium salt,[5] and 4-((trimethylsilyl)ethynyl)benznene (TMS) diazonium salt[6] were prepared and purified according to published procedures, and 4-((triisopropylsilyl)ethynyl)aniline (TIPS) was synthesized as described previously [7].

*General procedure for synthesis of the azides.* The mixture of the corresponding bromine terminated precursor and sodium azide in DMF was stirred at room temperature for 12 h. After all starting material was converted in to azide (confirmed by GC-MS) the reaction mixture was extracted with DCM, washed with water and dried over $MgSO_4$. Purification was done by silica-gel column chromatography with (DCM). The desired products were obtained in almost quantitative yields.

**Azidomethylferrocene.** Prepared according to literature procedure[1] from ferrocenemethanol in 80% yield, $^1H$ NMR (600 MHz, $CDCl_3$) δ 4.24 (t, 2H, J=1.8 Hz), 4.20 (t, 2H, J=1.8 Hz), 4.17 (s, 5H), 4.12 (s, 2H).

**1-Azidohexylferrocene.** Prepared according to literature procedure[2] from 1-bromohexylferrocene in 98% yield. $^1H$ NMR (600 MHz, $CDCl_3$) δ 4.09 (s, 5H), 4.04 (m, 4H), 3.26 (t, 2H, J=6 Hz), 2.33 (t, 2H, J=6 Hz), 1.60 (t, 2H, J=6 Hz), 1.51 (t, 2H, J=6Hz), 1.32-1.42 (m, 4H).

**1-Azidooctane.** Prepared according literature procedure[3] from 1-bromooctane in quantitative yield, $^1H$ NMR (300 MHz, $CDCl_3$) δ 3.25 (t, 2H, J=6.9 Hz), 1.56-1.62 (m, 2H), 1.20-1.50 (m, 10H), 0.89 (t, 3H, J=6.9 Hz).

**1-Azidododecane.** Prepared according to literature procedure[3] from 1-bromododecane in quantitative yield. $^1H$ NMR (600 MHz, $CDCl_3$) δ 3.25 (t, 2H, J=7.2 Hz), 1.55-1.68 (m, 2H), 1.20-1.42 (m, 20H), 0.88 (t, 3H, J=7.2 Hz).

**1-Azidohexadecane.** Prepared according to literature procedure[3] from 1-bromohexadecane in quantitative yield. $^1H$ NMR (600 MHz, $CDCl_3$) δ 3.25 (t, 2H, J=7.2 Hz), 1.55-1.68 (m, 2H), 1.20-1.42 (m, 26H), 0.88 (t, 3H, J=7.2 Hz).

## Fabrication of PPF

Pyrolyzed photoresist films (PPF) were made on thermally oxidized silicon chips (18 mm × 13 mm, 350 nm oxide layer) as described previously[8]. Briefly, the silicon chips were first cleaned with sequential immersion and sonication in acetone, IPA, and deionized Milli-Q water (TOC < 5 ppb) for 20 minutes each. The substrates were then dried in a nitrogen stream. Positive photoresist (AZ P4330-RS, AZ Electronic Materials) was spin-coated onto clean substrates at 500 rpm for 10 s followed by 6000 rpm for 50 s and soft baked at 95 °C for 10 min in air. For junction fabrication, photoresist was patterned photolithographically (500 W Hg arc lamp, 120 s) and developed in a (1:2 v/v) mixture of AZ400K developer and Milli-Q water to form four parallel 0.5 mm wide stripes. For XPS, UPS and AFM analyses, blanket sheets of PPF were used. The photoresist was finally pyrolyzed by heating the samples in a tube furnace to 1025 °C under a constant flow of forming gas (5% $H_2$ in $N_2$) to form PPF.

## Modification of PPF

PPF films were modified by electrochemical reduction of diazonium ions to form the desired molecular layers as primer layers for the second modification step via click chemistry. The PPF was the working electrode in a conventional three electrode setup with a platinum wire as auxiliary electrode and $Ag/Ag^+$ (0.01M $AgNO_3$ in ACN) reference electrode. The $Ag/Ag^+$ reference electrode was calibrated against the redox potential of ferrocene. The redox potential of ferrocene is centered at ~87mV versus the $Ag/Ag^+$ reference electrode. The electroreduction step was performed in a 1 mM solution of the diazonium salt with 0.1 M tetrabutylammonium hexafluorophosphate as supporting electrolyte in ACN. Electroreduction was performed by sweeping the electrode potential in an argon-degassed solution from +0.3 V to -0.65 V versus $Ag/Ag^+$ for one cycle at a scan rate of 0.1 $Vs^{-1}$ for EB diazonium ion and from +0.4 V to -1 V versus $Ag/Ag^+$ for 5 cycles at a sweep rate of 0.05 $Vs^{-1}$ for TMS diazonium ion. TIPS diazonium ions were generated in-situ: 30mg of sodium nitrite in 1mL water was added to a 1 mM solution of TIPS amine in 0.1 M tetrabutylammonium hexafluorophosphate in ACN and stirred for 20 min. The solution was cooled to 0 °C in an ice bath and degassed with argon for 20 min. Then 0.1 mL of concentrated $H_2SO_4$ was added and the mixture was stirred for another 5 min before scanning the potential from +0.4 V to -1 V versus $Ag/Ag^+$ for five cycles at a sweep rate of 0.05 $Vs^{-1}$. After surface modification, samples were rinsed thoroughly with benzene, THF and ACN and dried with nitrogen. The same procedures were conducted on glassy carbon electrodes for comparison. GC electrodes were polished successively with 1.0, 0.3, and 0.05 μm alumina/Milli-Q water slurries on microcloth pad. The GC electrodes were next rinsed with Milli-Q water and sonicated in activated carbon/ACN solution [9]. Finally the GC electrodes were rinsed with IPA and ACN and dried with a nitrogen stream before modification.

## Secondary modification with click chemistry

A Teflon sample holder was used to hold the chips during the "click" reaction. The click reaction (Cu(I)-catalyzed Huisgen 1,3-dipolar cycloaddition) between deprotected acetylene moieties on the surface and various azides in solution was used for further modification. For MeFc, 1-(azidomethyl)-4-methylbenzene (MePh), and HxFc, 1:1 (v/v) water:ethanol solutions of $CuSO_4$ (0.5 mM) and dropwise added L(+)-ascorbic acid (2 mM) were stirred and bubbled with argon for 16 hours in the presence of 0.01 mM of the corresponding azide and EB modified PPF substrates.[7] The click modified samples were rinsed with THF and water and immersed in 10 mM EDTA for 1 min and 1 M ammonium hydroxide solution for 30 s to remove copper residues. Finally the modified chips were rinsed with water, acetone and ACN and dried with nitrogen gas. For $C_8$ azide, $C_{12}$ azide, and $C_{16}$ azide, 4:1 (v/v) DCM:ACN solutions of tetrakis(acetonitrile)copper(I) tetrafluoroborate (0.2 mM) and TEA (2.5 mM) were stirred and bubbled with argon gas for 18 hours in the presence of 2.5 mM of the corresponding azide and EB modified PPF substrates. The samples were then rinsed with THF, acetone and ACN and dried with nitrogen gas.

## Tops contact deposition

Large area cross-bar junctions (~0.0013 $cm^2$) were fabricated by electron-beam deposition of carbon (10 nm) and gold (15 nm) top contacts through the openings in a shadow mask oriented perpendicular to the click modified PPF stripes in an electron-beam evaporator (Kurt J. Lesker PVD75) at a typical chamber pressure of $<5 \times 10^{-6}$ Torr [10]. The deposition rates for the top contacts were 0.01 nm/s for evaporated-carbon (e-C) and 0.05 nm/s for gold. E-beam deposited carbon has been described previously for electrochemistry [11] and molecular junctions [10], and exhibits metallic behavior and a resistivity of about 0.015 Ω.cm.

## Electrochemical measurements

The patterned PPF blanket sheets modified with EB and MeFc or HxFc bilayers were used to verify the electro-activity of the attached ferrocene and to determine the coverage of the immobilized ferrocene. Modified PPF samples were first rinsed with ACN and dried with a stream of nitrogen gas. The coverage measurements were done in a three electrode arrangement with modified PPF electrode as working electrode, a platinum wire as counter electrode and $Ag/Ag^+$ as reference electrode using an ethanolic solution of 0.1 M $LiClO_4$ as supporting electrolyte. We used the peak area of oxidation peaks at low scan rates for coverage calculations.

## XPS

X-ray photoelectron spectroscopy analyses were acquired with the AXIS 165 spectrometer equipped with a monochromatic Al Kα source (1486.6 eV).

## UPS

Ultraviolet photoelectron spectra were acquired with a Kratos Ultra spectrometer with a He I source (21.21 eV).

## Electronic measurements

Electrical characterization of molecular junctions was carried out using a Keithley 2602A in four-wire configuration[12]. The four wire configuration was used to correct for ohmic losses in contacts and leads. All the voltages reported in this work are PPF relative to the Au top contact. For temperature variation, a Janis ST-500-1 cryogenic probe station cooled with liquid nitrogen was utilized. The chamber was pumped to < 10-4 torr before lowering the temperature and acquisition of J-V data. The temperature was varied between 100-400 K and J-V curves were collected every 10 K.

Supporting Figures:

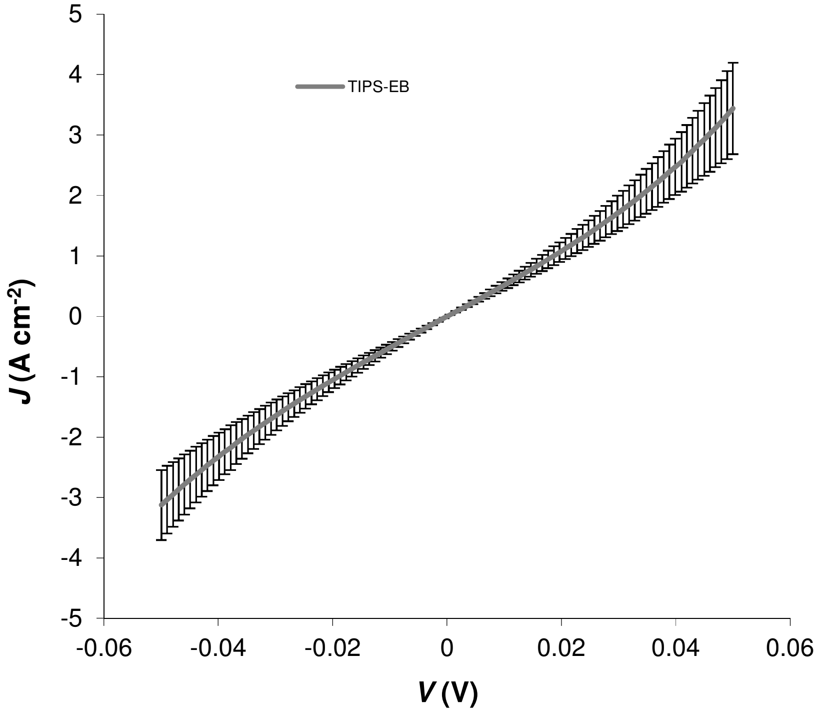

***Figure S1.*** J-V curve for PPF/TIPS-EB/e-C/Au junctions, without deprotection of the silane group.

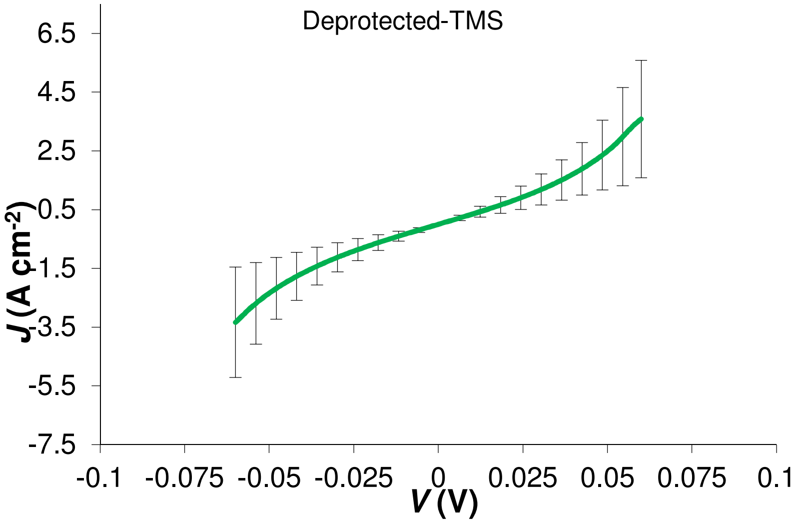

***Figure S2.*** J-V response for PPF/TMS-EB /e-C/Au molecular junctions, with deprotection of the TMS-EB layer before e-C deposition

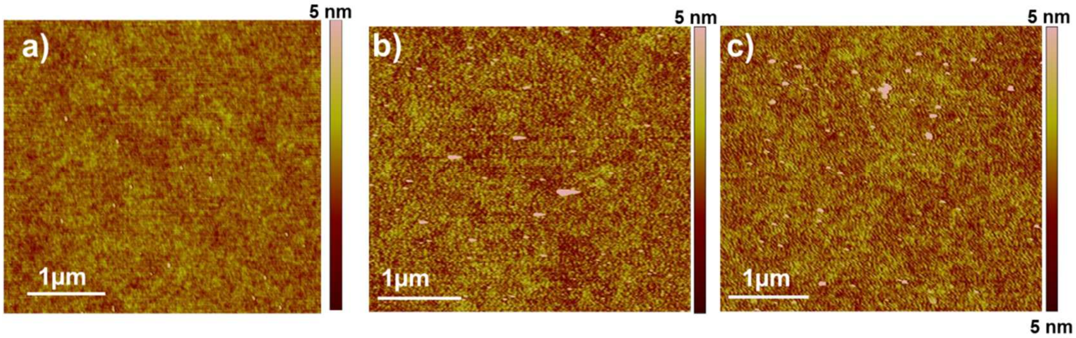

***Figure S3.*** AFM images for unmodified PPF surfaces (a), PPF modified with EB (b), and PPF modified with EB-MeFc (c). RMS roughnesses were 0.26, 0.43 and 0.51 nm, respectively.

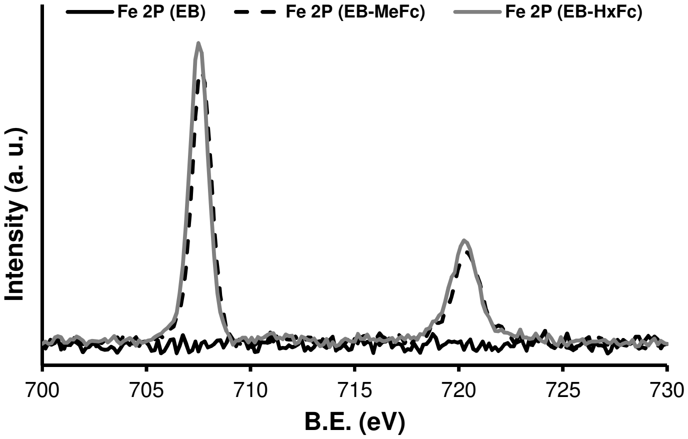

***Figure S4.*** $Fe_{2p}$ XPS spectra of PPF substrates modified with EB before and after Click chemistry with azidomethylferroccene and azidohexylferrocene.

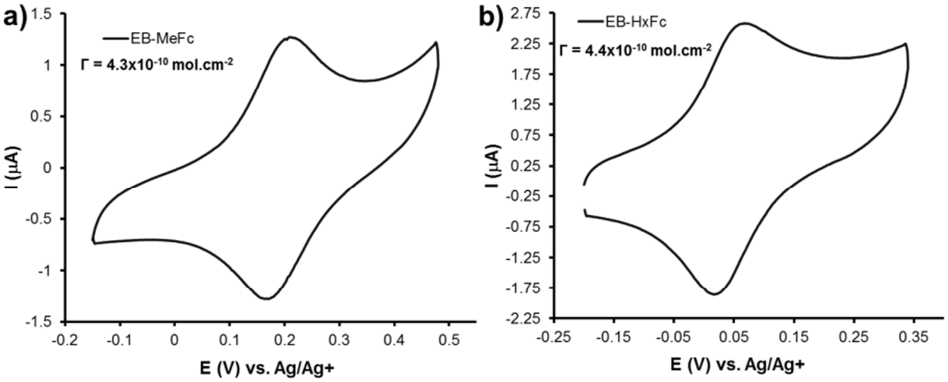

***Figure S5.*** Cyclic voltammogram in ethanol + 0.1 mol.L$^{-1}$ $LiClO_4$ of modified-PPF (EB-PPF) electrode after click chemistry with azidohexylferrocene (a) and azidomethylferrocene (b). Scan rate = 5 mV/s.

| Samples | # of junctions | $R_a$, nm | Yield | $RSD_{0.1\ V}$ |
|---|---|---|---|---|
| EB (2.2 ± 0.5 nm) | 16 | 0.426 | 14/16 | 25.8 % |
| EB-MePh(3.3 ± 0.4 nm) | 16 | 0.513 | 14/16 | 10.2% |
| EB-MeFc (3.4 ± 0.6 nm) | 16 | 0.437 | 16/16 | 21.3 % |
| EB-HxFc(3.9 ± 0.7 nm) | 16 | 0.508 | 15/16 | 6.70 % |
| *Alkane Series* | | | | |
| EB (2.6 ± 0.5 nm ) | 8 | 0.68 | 8/8 | 13.6 % |
| EB-C8 (3.00 ± 0.6 nm) | 8 | 0.49 | 8/8 | 1.18 % |
| EB-C12 (3.30 ± 0.6 nm) | 8 | 0.44 | 8/8 | 4.80 % |
| EB-C16 (3.78 ± 0.5 nm) | 8 | 0.46 | 8/8 | 6.40% |

**Table S1.** Yield and reproducibility of EB-based junctions with and without coupling to different azides by click chemistry. $R_a$ is the root mean square (RMS) roughness from AFM for the indicated surfaces before top contact deposition. The relative standard deviations calculated for the junctions illustrated in Figure1 and Figure 2 of the main text. The overall yield for the fabricated devices is 92% and 100% for the ferrocene and alkane series, respectively.

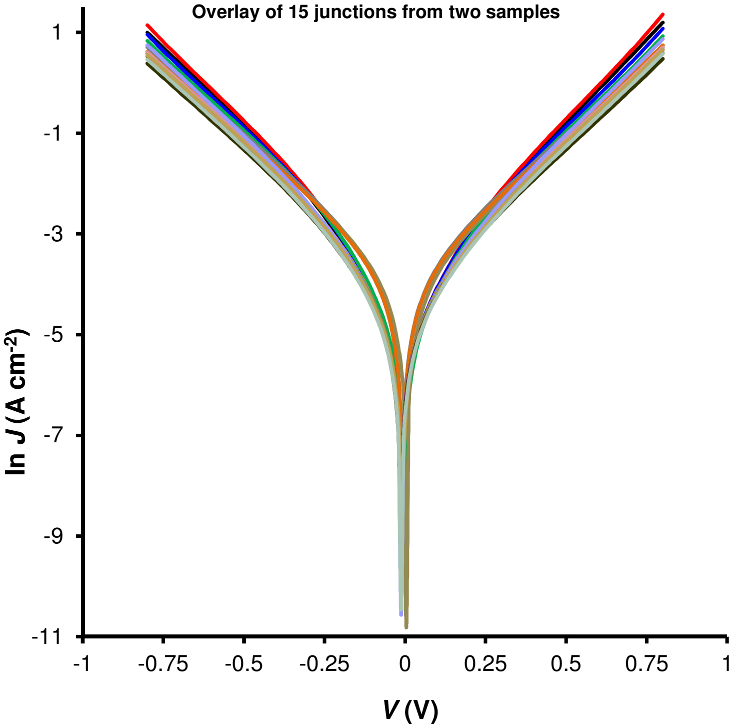

***Figure S6.*** Overlay of 15 Junctions from two samples composed of PPF/ EB coupled to hexylferrocene by click chemistry followed by top contact deposition.

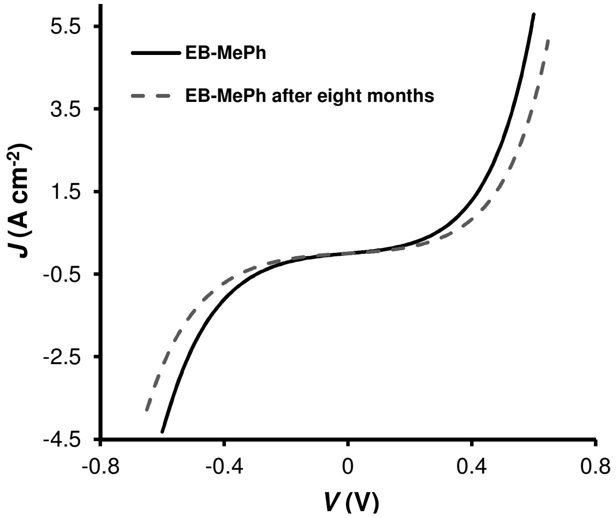

***Figure S7***. Overlay of J-V curves for a EB-MePh junction after eight months exposure to ambient air.

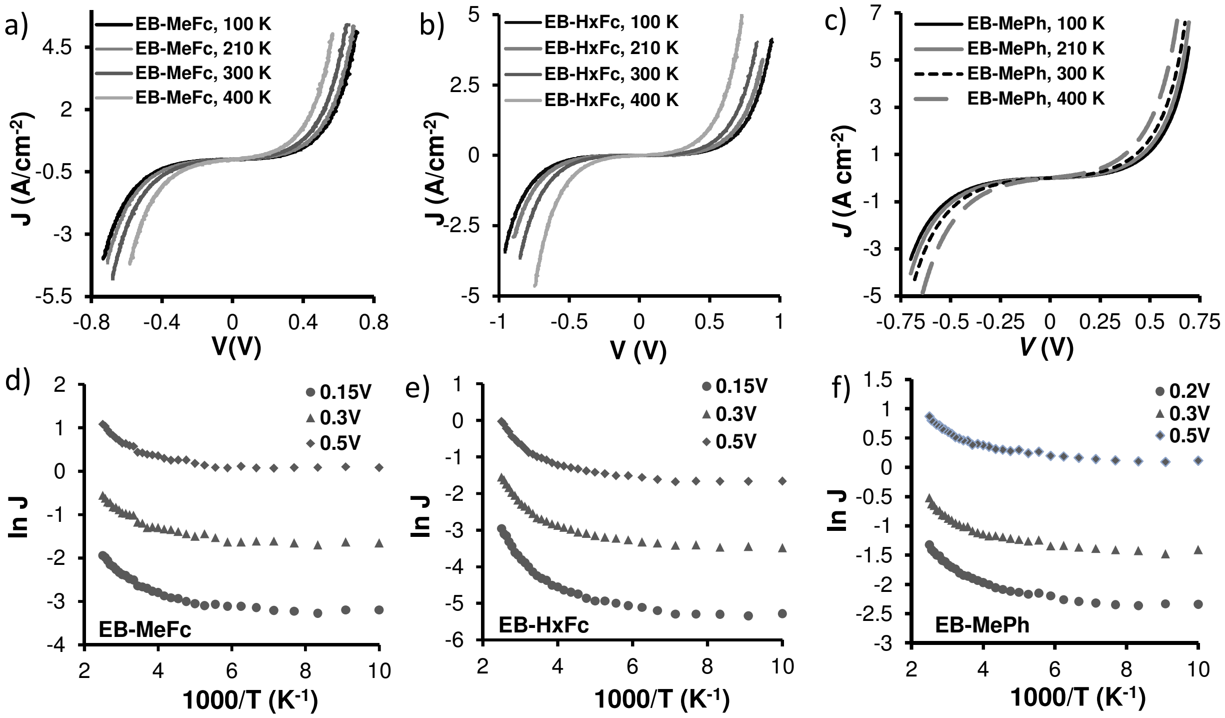

***Figure S8.*** (a-c) *J-V* curves for PPF/molecule/e-C/Au junctions containing ferrocene and methyl-phenyl layers, as indicated, in the temperature range from 100-400 K. (d-f) Arrhenius plots at different bias voltages.

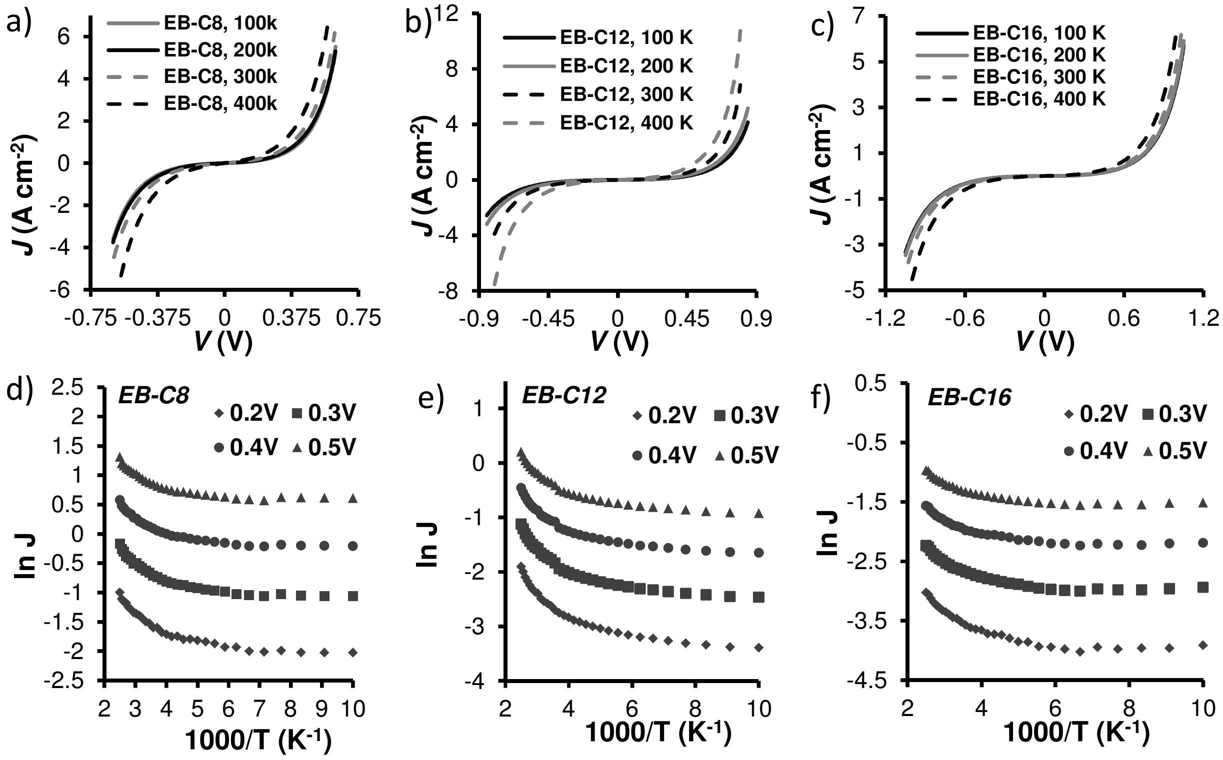

***Figure S9.*** (a-c) A series of *J*-*V* curves in the temperature range from 100-400 K. (d-f) Arrhenius plots at different biases.

| | 100 – 210 K | | 300 – 400 K | |
|---|---|---|---|---|
| | 0.2 V | 0.5 V | 0.2 V | 0.5 V |
| **EB-MeFc** | 3.70 | 1.60 | 56.2 | 54.4 |
| **EB-HxFc** | 7.93 | 4.80 | 114 | 94.8 |
| **EB-MePh** | 4.21 | 3.43 | 44.0 | 35.2 |
| **EB-$C_8$** | 3.90 | 1.20 | 47.0 | 36.3 |
| **EB-$C_{12}$** | 6.50 | 4.20 | 68.2 | 53.1 |
| **EB-$C_{16}$** | 1.60 | 0.80 | 46.2 | 32.4 |

***Table S2***. Arrhenius slopes for various junctions of EB modified by click chemistry with MeFc, MePh, HxFc, $C_8$, $C_{12}$, and $C_{16}$.

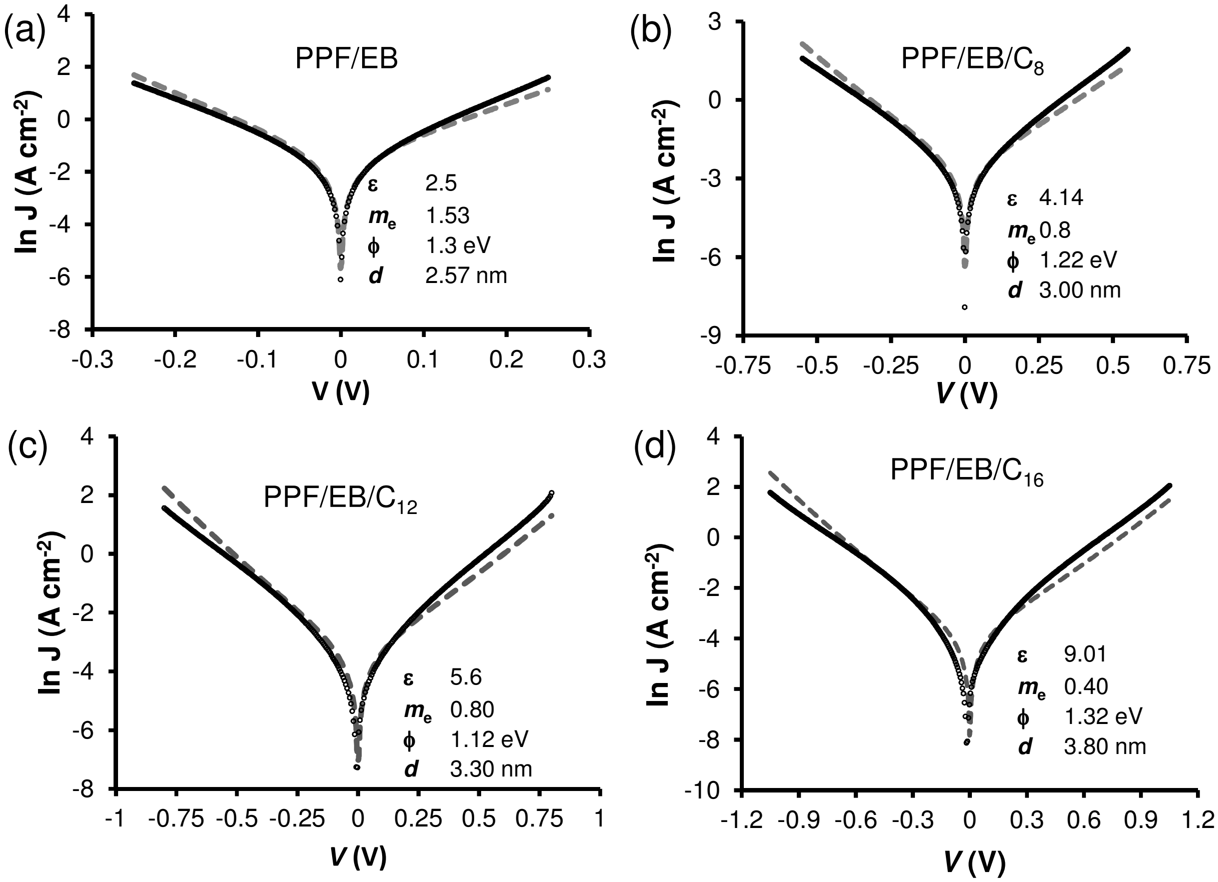

***Figure S10***. J-V curves for different t EB-based junctions fit to the Simmons model as described previously[13]. The black dots are the experimental data, while the gray broken lines are the results of the full Simmons model, where the parameters obtained are indicated.

## Measurement of Molecular Layer Thickness

Molecular layer thicknesses were determined with AFM “scratching” as described previously [14], with a more detailed statistical analysis described below. In contact mode, an area of 1µm x 1µm was scanned under a set point of (0.25 V). As a result the molecular film was removed without scratching the PPF leaving a trench, which is used to determine the height of the molecular layer after scanning a larger area (5µm x 5µm) of the same spot in tapping mode (figure S11). The molecular layer thickness was determined as the difference in heights between the bottom of the trench and the top of the surrounding molecular layer. Two histograms, for the heights of the trench and the surrounding area were fit by two different Gaussian functions (figure 12). Thicknesses stated in main text are the difference of the centers of the Gaussian distribution, with the uncertainty in thickness stated as the quadrature addition of the two best-fit $\sigma$ values.

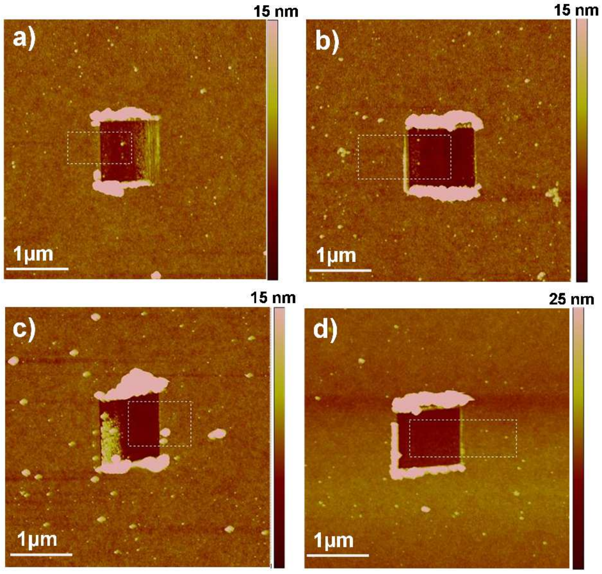

***Figure S11.*** AFM images of trenches made in molecular layers of EB (a), EB-MeFc (b), EB-MePh (c), and EB-HxFc (d) on carbon (PPF).

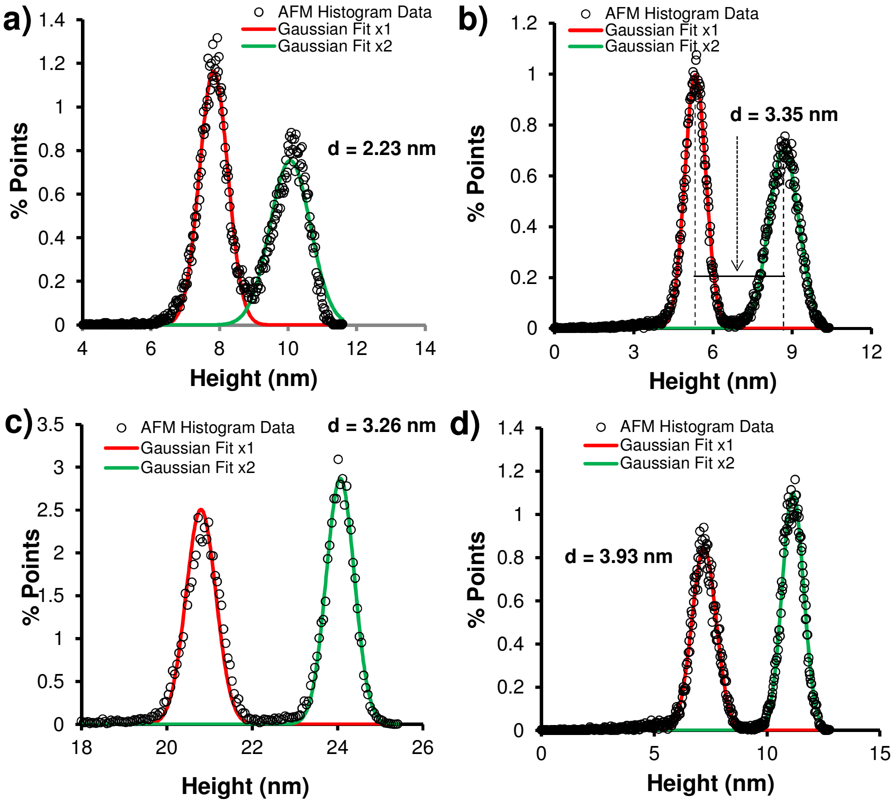

***Figure S12.*** Fitting of the AFM height data generated as a histogram from the images shown in Figure S11, i.e. EB (a), EB-MeFc (b), EB-MePh (c), and EB-HxFc (d)

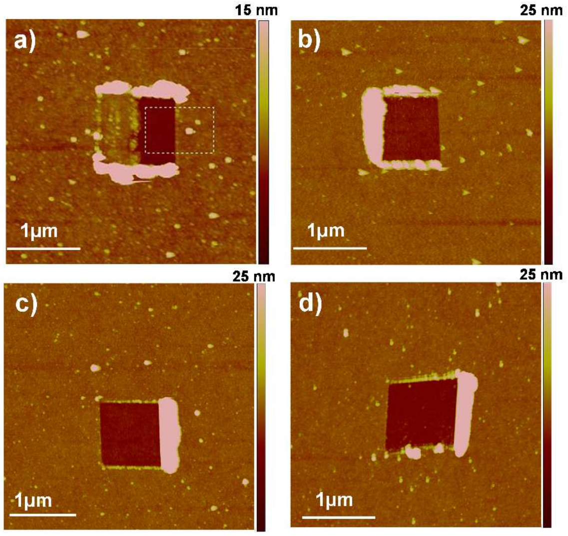

***Figure S13.*** AFM images of trenches made in molecular layers of EB (a), EB-C8 (b), EB-C12 (c), and EB-C16 (d) on carbon (PPF).

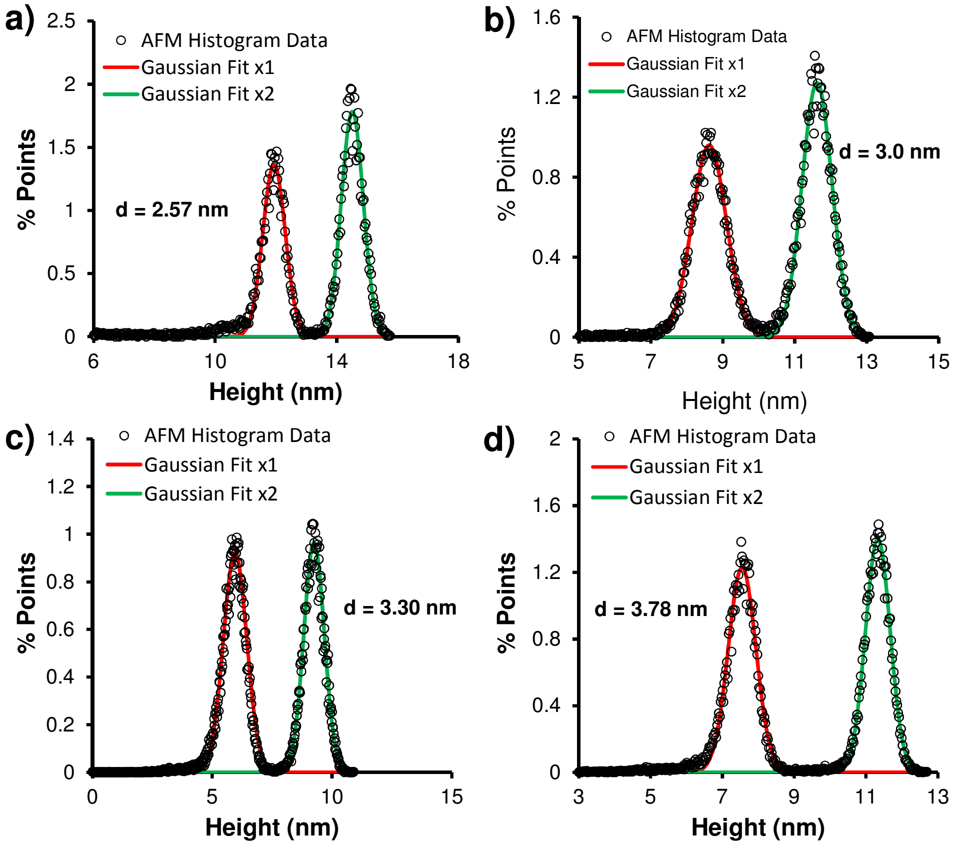

***Figure S14.*** Fitting of the data generated as a histogram from the AFM data shown in Figure S13, i.e. EB (a), EB-C8 (b), EB-C12 (c), and EB-C16 (d).

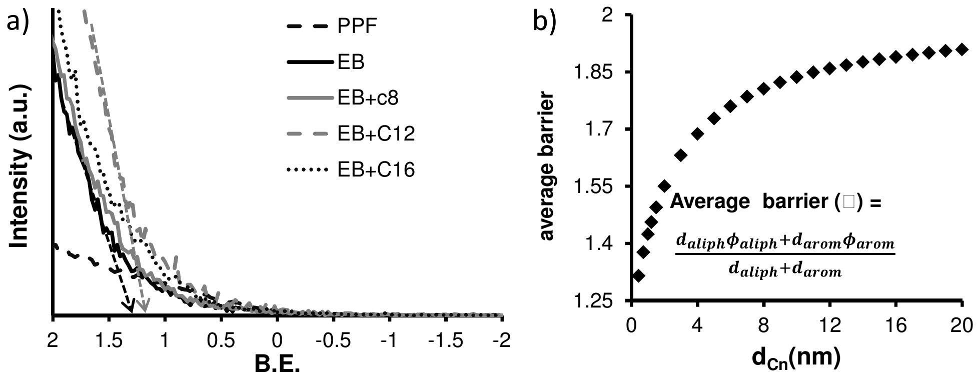

***Figure S15.*** (a) Overlay of UPS spectra for EB junctions before and after click reaction with azidoalkanes (a); the spectra are presented near the PPF Fermi level to determine the $E_{HOMO,onset}$. (b) Plot of the calculated average barrier for junctions made out of EB (2.57 nm) and increasing thiknesses of coupled alkanes. The inset equations was used to calculate the average barrier, where □$_{aliph}$ = 1.2 eV and □$_{arom}$ = 2.0 eV.[15]

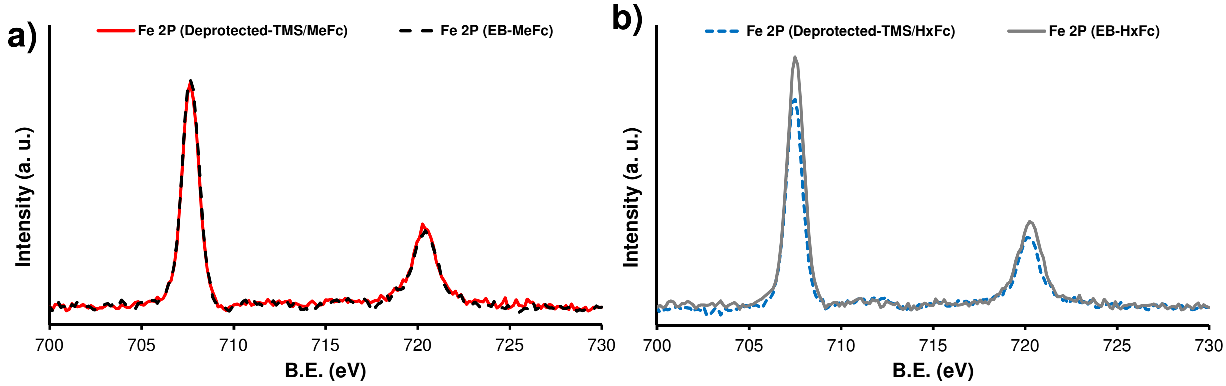

***Figure S16.*** $Fe_{2p}$ XPS spectra of methylferrocene (a), and hexylferrocene (b) coupled by click chemistry on EB (method 2) and deprotected-TMS (method 1).

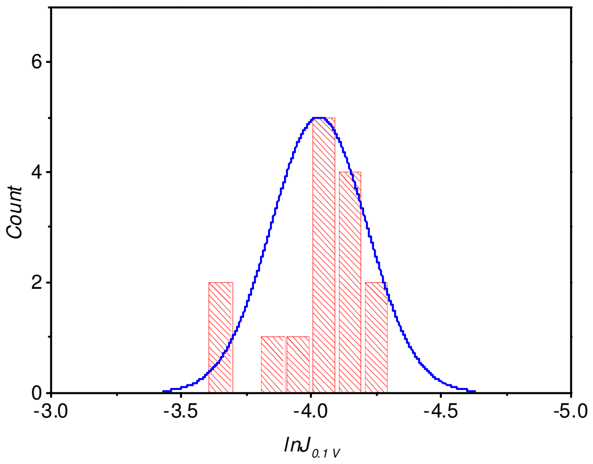

***Figure S17.*** Statistical distribution of ln *J* at 0.1 V for fifteen EB-HxFc junctions. Ordinate is the number of junctions exhibiting conductances at 0.1 V in a range of 0.1 ln units. Solid line is a Gaussian distribution for comparison.

| Sample | $E_{HOMO,\ onset}$ (eV) | $\phi_{Simmons}$ (eV) | $\phi_{average}$ (eV) |
|---|---|---|---|
| PPF/EB | 1.28 ±0.04 | 1.30 | 1.20 |
| PPF/EB/$C_8$ | 1.28 ±0.04 | 1.22 | 1.31 |
| PPF/EB/$C_{12}$ | 1.20 ±0.01 | 1.22 | 1.38 |
| PPF/EB/$C_{16}$ | 1.25 ±0.04 | 1.32 | 1.46 |

***Table S3.*** Values of the $E_{HOMO,onset}$ estimated from UPS measurements, barrier height from fitting the data to Simmons's model, and the average barrier calculated from coupling the EB layer with $C_8$, $C_{12}$, and $C_{16}$.

## References

(1) Casas-Solvas, J. M.; Vargas-Berenguel, A.; Capitán-Vallvey, L. F.; Santoyo-González, F.; *Organic Letters* **2004**, *6*, 3687-3690.

(2) Lee, Y.; Morales, G. M.; Yu, L.; *Angewandte Chemie - International Edition* **2005**, *44*, 4228-4231.

(3) Baek, S. Y.; Kim, Y. W.; Yoo, S. H.; Chung, K.; Kim, N. K.; Kim, J. S.; *Industrial and Engineering Chemistry Research* **2012**, *51*, 9669-9678.

(4) Lamani, M.; Prabhu, K. R.; *Angewandte Chemie - International Edition* **2010**, *49*, 6622-6625.

(5) Evrard, D.; Lambert, F.; Policar, C.; Balland, V.; Limoges, B.; *Chemistry - A European Journal* **2008**, *14*, 9286-9291.

(6) Leroux, Y. R.; Hapiot, P.; *Chemistry of Materials* **2013**, *25*, 489-495.

(7) Leroux, Y. R.; Fei, H.; Noël, J.-M.; Roux, C.; Hapiot, P.; *Journal of the American Chemical Society* **2010**, *132*, 14039-14041.

(8) Ranganathan, S.; McCreery, R. L.; *Analytical Chemistry* **2001**, *73*, 893-900.

(9) Ranganathan, S.; Kuo, T.-C.; McCreery, R. L.; *Analytical Chemistry* **1999**, *71*, 3574-3580.

(10) Yan, H.; Bergren, A. J.; McCreery, R. L.; *Journal of the American Chemical Society* **2011**, *133*, 19168-19177.

(11) Blackstock, J. J.; Rostami, A. A.; Nowak, A. M.; McCreery, R. L.; Freeman, M.; McDermott, M. T.; *Analytical Chemistry* **2004**, *76*, 2544-2552.

(12) Ru, J.; Szeto, B.; Bonifas, A.; McCreery, R. L.; *ACS Applied Materials and Interfaces* **2010**, *2*, 3693-3701.

(13) Bergren, A. J.; McCreery, R. L.; Stoyanov, S. R.; Gusarov, S.; Kovalenko, A.; *Journal of Physical Chemistry C* **2010**, *114*, 15806-15815.

(14) Anariba, F.; DuVall, S. H.; McCreery, R. L.; *Analytical Chemistry* **2003**, *75*, 3837-3844.

(15) Sayed, S. Y.; Fereiro, J. A.; Yan, H.; McCreery, R. L.; Bergren, A. J.; *Proceedings of the National Academy of Sciences* **2012**, *109*, 11498-11503.